Injury biomechanics in aircraft crash-landing reconstruction

Geoffrey T. Desmoulin*, Theodore E. Milner, Marc-André Nolette and Kevin G. Bird

GTD Scientific Inc.,
2037 MacKay Avenue,
Vancouver, BC, V7P 2M8, Canada
Email: gtdesmoulin@gtdscientific.com
Email: temilner@gtdscientific.com
Email: manolette@gtdscientific.com
Email: kgbird@gtdscientific.com
*Corresponding author

Elvis Cepuš

R J Waldron and Company,
110 – 5920 Number 2 Road,
Richmond, BC, V7C 4R9, Canada
Email: elvis@rjwaldronco.com

Abstract: Despite significant progress in aircraft crashworthiness, unexpected and oddly serious injuries are sometimes seen in otherwise survivable incidents. In one such case, a small fixed-wing aircraft crash-landed on a sand bar before flipping onto its roof, causing a spinal cord injury to one of four occupants while others only suffered minor injuries. An injury biomechanics investigation revealed that the L1 wedge fracture suffered by the victim was associated with axial compression combined with anterior flexion of the spine which would likely have been caused by the plane's flipping motion. Calculations revealed that these stresses would only have been present at the end of the flip when the plane landed on its wing and the victim impacted the ceiling of the aircraft upon the failure of his seatbelt. Further inspection then revealed a flaw in the seatbelt's attachment which may have caused it to come undone during the landing.

Keywords: injury biomechanics, fixed-wing aircraft, crashworthiness, seatbelt, forensics.

Reference to this paper should be made as follows: Desmoulin, G.T., Milner, T.E., Nolette, M-A., Bird, K.G. and Cepuš, E. (2021) 'Injury biomechanics in aircraft incident reconstruction', *Int. J. Forensic Engineering*, Vol. 5, No. 1, pp.72–85.

Biographical notes: Geoffrey T. Desmoulin, PhD, R.Kin., P.L.Eng., is the Principal of GTD Scientific Inc. (www.gtdscientific.com). GTD Scientific offers biomechanical consulting services on behalf of clients throughout North America, as well as abroad. Focused practice areas include injury biomechanics, incident reconstruction, and physical testing with a subspecialty in the Science of Violence®. GTD Scientific has been retained in significant complex injury litigation cases involving municipal police departments,

Copyright © 2021 Inderscience Enterprises Ltd.

the National Basketball Association, TASER International, Cornell University, and a Sprint Class race car incident, to name just a few examples.

Theodore E. Milner, PhD, is Professor Emeritus of McGill University and Senior Scientist at GTD Scientific, Inc. He was a Professor in the Department of Kinesiology and Physical Education at McGill University from 2008–2020, Professor in the School of Kinesiology at Simon Fraser University from 1992 to 2007 and Professor in the Institute of Biomedical Engineering at the University of Montreal from 1986-1992. He was a research fellow in the Rehabilitation Engineering Lab at ETH-Zurich from 2014 to 2016 and a visiting researcher at the Advanced Telecommunications Research Institute International from 2000 to 2007. His research has focused on the areas of human motor control, biomechanics and neurorehabilitation.

Marc-André Nolette, MSc, is an Injury Biomechanist at GTD Scientific Inc. He received a Master's degree in Biomedical Physiology from Simon Fraser University in 2012 and a Bachelor's degree in Mechanical Engineering from Universté de Sherbrooke in 2009.

Kevin G. Bird holds a degree in Materials Engineering from the University of British Columbia. He is an Associate at GTD Scientific Inc. (www.gtdscientific.com). His responsibilities include incident reconstruction and all of GTD Scientific's materials science needs.

Elvis Cepuš, RJ Waldron & Co., is an internationally recognised firm specialising in Aviation Accident Investigation and Failure Analysis. He has 15 years of experience in engineering failure analysis, has conducted approximately 1000 investigations, and is an Adjunct Professor at UBC. His background blends mechanical engineering, metals and materials engineering, composite materials, design, fracture mechanics and fatigue analysis.

1 Introduction

Increasing survivability of aircraft emergency landings and crashes has long been a focus of the aviation research community (De Haven, 1953; Hasbrook, 1969). This research has vastly improved the crashworthiness of aircraft and therefore, the outcome for occupants (Greer et al., 1964). However, constant improvement remains an important goal of aircraft design (Snyder, 1975; Schwinn, 2014) as avoidable injuries are still seen in emergency crash landings today.

To achieve this, incidents have to be understood in order to improve upon the unexpected failures. A case involving a light aircraft crash landing on a sand bar was recently involved in litigation after an occupant suffered a spinal injury during the incident.

This publication aims to demonstrate how reconstruction methodology can be used to identify the cause of the injury when little information is available. To do so, a real-life case has been anonymised and used to show the application of such a reconstruction methodology.

2 Case presentation

2.1 Incident

This incident involves a single-engine general aviation aircraft with fixed landing gear suffering a total loss of engine power over a remote region of north western Canada. The aircraft eventually crash landed on a sand bar which led at least one occupant to suffer serious injuries.

The pilots and other occupants later described the crash landing as follows. The back left wheel of the plane was the first to touch the ground and began rolling along the sand bar. The front nose wheel dug into the soil, causing the nose strut to fracture at the point of attachment to the wheel after which the plane bounced off the ground without its front wheel. When the plane landed again the strut dug into the sand bar. The plane began decelerating as the damaged landing gear plowed a furrow through the soft soil. The plane eventually flipped forward and landed on its wing.

During the incident, the seatbelt of one passenger, sitting in the second row, detached from one of its lateral attachment points, which caused the passenger to come to rest on the ceiling of the inverted plane. The passenger in question described feeling a sharp pain in his lower back, which soon became unresponsive to his efforts to move. The occupants were later rescued and the passenger of interest was diagnosed with an anterior wedge fracture of his L1 vertebra with 25% compression.

It is important to note that the occupant's seatbelt was secured at the time of the crash and that it did not show any visible damage after becoming undone (Figure 1). The seatbelt in question was a standard two-point lap seatbelt with a metal buckle and two lateral carabiner type attachments.

Figure 1 Seatbelt of the passenger of interest (top) from the incident and seatbelt (bottom) of other occupant (see online version for colours)

2.2 Injury analysis

The injured passenger was later diagnosed with an anterior wedge compression fracture of his L1 vertebra. Imagery showed a 25% decrease in the height of the anterior body of the vertebrae. Despite a slight deterioration in the month after the accident, this injury was considered stable, as the decrease in height was less than 50%, which is typical of this injury (Kim et al., 2015; Ghobrial, 2016; Yoganandan et al., 2014).

Anterior wedge fractures (Figure 2) are caused by axial compression combined with anterior flexion of the spine (Ghobrial, 2016; Yoganandan et al., 2014). Forward flexion creates localised compression loading on the anterior structure of the spine (Yoganandan et al., 2014). The combination of axial compression and localised compression creates a distinct wedge-shaped fracture (Yoganandan et al., 2014). There are two principal mechanisms of applying a combination of flexion and compression loads to the spine. The first mechanisms is a load applied axially at the pelvis while the centre of mass of the torso is bent anteriorly in front of the applied load as depicted in Figure 3(a) (Yoganandan et al., 2014).

Figure 2 Anterior wedge fracture showing a decrease in vertebral height on the anterior surface of the vertebrae (see online version for colours)

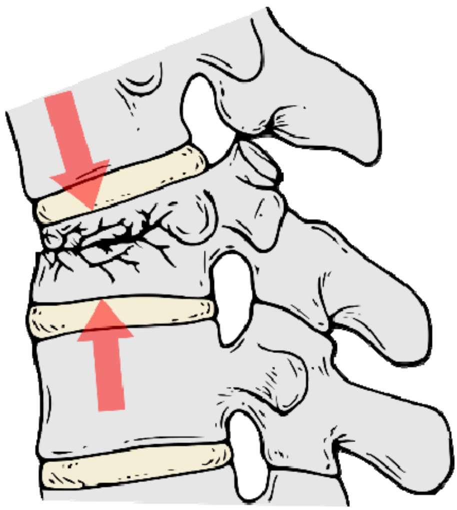

Source: Old and Calvert (2004)

The second mechanism is an axial load applied anteriorly to the centre of rotation of the injured vertebral segment as depicted in Figure 3(b) (Yoganandan et al., 2014).

Figure 3 Anterior wedge fracture mechanism of injury with an axial load applied: (a) posterior and (b) anterior to the centre of gravity of the torso

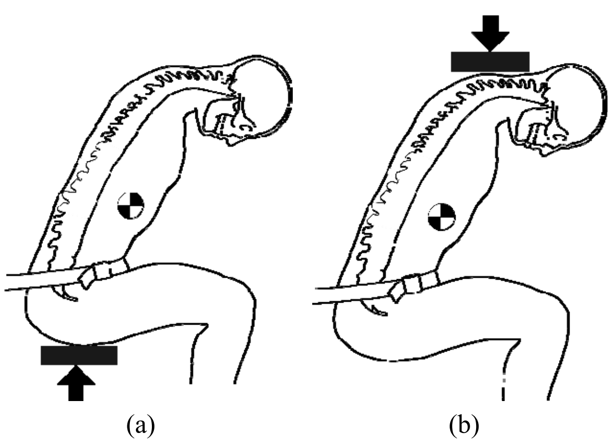

The majority of flexion-compression injuries occur where the thoracic spine meets the lumbar spine. This is referred to as the thoracolumbar junction and it spans the T11 and the L2 vertebrae (Yoganandan et al, 1988).

Studies investigating anterior wedge fracture tolerance typically analyse fractures of multiple vertebrae. Yoganandan et al. (1988) performed drop testing on in-vitro human spine specimen segments of various lengths and recorded the axial failure load and the flexion moment at the time of failure. Myklebust et al. (1983) induced wedge compression fractures in the spine of multiple specimens including whole cadavers by loading the upper spine to induce flexion-compression. Although flexion-compression injuries typically occur at the thoracolumbar junction, not all fractures reported in these studies occur between the T11 and L2 vertebrae (Yoganandan et al, 1988; Myklebust et al, 1983). With the injury of interest being located at L1, only the load to failure for vertebrae between T12 and L2 were selected to biomechanically characterise this injury. The applicable results of the Yoganandan et al. study and the Myklebust et al. study were combined to create a mean tolerance for L1 compression fractures based on the data in Table 1.

Table 1 Combined tolerance for anterior wedge fractures

	Vertebrae Level	*Fracture Load (N)*
Yoganandan et al. (1988)	L1	1730
	T12	1113
	T12	4444
	T12	801
	T12	1330
	T12	5560
	T12	5275
Myklebust et al. (1983)	L1	1730
	T12	444
	T12-L1	1330
	L2	2750
	Average	2410
	Standard Deviation	1838

The mean failure load was 2410 ± 1838 N. Going forward, this force can be used to describe the 50% probability of injury for the case under investigation.

3 Methodology

In an effort to describe and understand the dynamics of the incident, information from the occupants' testimonies and accident scene photos have been combined to create a model of the crash landing depicted as the 4 phases shown in Figure 4.

Figure 4 Four phases of the crash landing

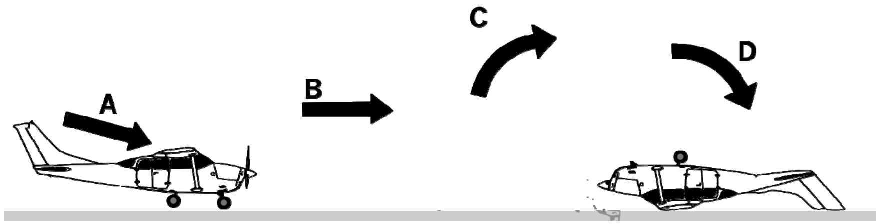

The first phase is the initial contact with the ground, which ended when the nose strut broke and the front wheel assembly detached. The second phase is the second contact with the ground when the nose strut dug into the sand bar and the resistive force between the fuselage and the ground horizontally decelerated the plane and caused it to rotate clockwise or forward. The third phase begins when the plane stopped sliding forward but continued to rotate clockwise over its nose. The final phase is where the plane landed on its wing and tail at the end of the clockwise rotation, i.e., the end of the forward flip. Using the information available, the risk of anterior wedge fracture was evaluated in the appropriate phases.

3.1 Phase A: initial contact

In the initial phase of the crash, the plane touched down on the sand bar. It first made contact with its rear left wheel. This can be observed in a photo taken at the scene (Figure 5), as the leftmost track in the soil is closer to the camera, which is facing in the direction of travel of the aircraft at the time of impact.

Figure 5 Evidence of gear initial contact with ground (see online version for colours)

The second point of contact with the ground presumably involved the nose wheel, while the right wheel hit last. Although the middle and right tracks seen in Figure 5 appear to start at a similar distance from the camera, the front wheel is located approximately 5 feet in front of the back wheels of the aircraft. Therefore, it can be assumed that the plane's wheels touched down from left to right in turn.

Upon contact, the front landing gear was damaged in such a way that the front wheel assembly broke from the nose strut. This is known because the wheel was found a short distance beyond the initial point of contact of the front wheel with the ground (Figure 5).

3.2 Phase B: second contact

Following this initial contact with the ground, the plane bounced back into the air and landed again but without the front wheel. The nose strut dug into the ground and the plane began to decelerate.

3.3 Phase C: deceleration and flip initiation

As the plane decelerated, the front end plowed a furrow in the soil (Figure 6). Measurements of the height of the cockpit and wingspan, taken from the photo in Figure 6, were replicated in photos of objects of matched dimensions taken at different distances with an exemplar camera. From this matching process, it was determined that the photo in Figure 6 would have been taken from approximately 30 m in the front of the plane. Since the photographer was standing at the start of the furrow, we estimated that the plane slid for 30 m before its forward motion terminated. During this time, the horizontal ground reaction force, applied by the soil to decelerate the plane, created a clockwise torque around the plane's centre of gravity which overcame the counter clockwise torque created by the vertical ground reaction force applied by the soil due to the weight of the plane. This created clockwise angular acceleration around the centre of gravity, causing the entire plane to begin to rotate around its contact point with the ground.

Figure 6 Furrow created by the damaged landing gear (see online version for colours)

The clockwise angular acceleration continued until the horizontal motion of the front of the plane had stopped. By this point it had acquired sufficient angular momentum to continue its clockwise rotation, although with decreasing angular velocity.

3.4 Phase D: plane flip and impact

When the plane's centre of gravity reached a point where it was vertically aligned with the front of the plane, the torque applied by the vertical ground reaction force reversed direction such that the plane tipped over backwards and began to accelerate again in the clockwise direction, continuing to rotate at increasingly higher angular velocity until the leading edge of the wing hit the ground, slowing its rotation and eventually stopping when the tail hit the ground.

4 Analysis

4.1 Phase A: initial contact

According to the evidence and testimonies available, it appears that the initial contact with the ground was relatively mild and was unlikely to cause severe injuries if considered in isolation. Therefore, this analysis focuses on the subsequent phases of the incident.

4.2 Phase B: second contact

According to statements made by the passenger of interest, he remained in his seat during the first and second touchdowns, which indicates that his seatbelt was likely attached at the time.

The seatbelt restrains the passenger from leaving the seat but it is likely to cause the passenger's torso to lean forward during vertical impact. The force applied to the passenger during touchdown was not likely responsible for the L1 compression fracture. Mild impacts of this type, have been shown to cause what is referred to as a chance fracture (Kim et al., 2015; Yoganandan et al., 2014; Saber et al., 2017). Chance fractures occur through a combination of flexion and distraction forces on the spine.

Although chance fractures have a 50% probability of occurring at the thoracolumbar junction, the most significant indication of such an injury is manifested as horizontal splits in the transverse process and pedicles of the vertebrae (Huelke and Kaufer, 1975; Denis, 1984). The anterior wedging which occurred in the passenger of interest is not typical of chance fractures (Jones, 2017). Nevertheless, it has been reported in instances of car crashes, where vertical loads were also present (Huelke and Kaufer, 1975; Denis, 1984)

In the case of the injury under investigation, no damage was reported to the posterior aspect of the spine. This suggests that Phase B was not responsible for the injury sustained by the passenger.

4.3 Phase C: deceleration and flip initiation

As the front of the plane plowed through the soil, the plane's centre of gravity was subjected to clockwise angular acceleration. Passengers seated and restrained by their seatbelts would be subjected to the same angular acceleration. It is assumed that since the plane flipped, the horizontal deceleration was great enough to cause all of the plane's weight to be transferred to the front of the plane, where the nose strut is located. In this case, the angular acceleration can be represented by the following equation of motion.

$$\tau = mgR(\theta)\cos\theta + maR(\theta)\sin\theta = I\ddot{\theta} \tag{1}$$

Here the net torque, τ, is equal to the difference in the torque created by the weight, mg, and the torque created by the resistance of the soil, ma, where R is the distance from the centre of pressure to the plane's centre of gravity. The angle, θ, is the angle between R and the horizontal. On the right side of the equation, I, is the moment of inertia of the plane about a horizontal axis passing through the centre of gravity and parallel to the wing.

Photos of the damaged front landing gear, following the crash, suggest that it was buried right to its base as it plowed through the soil, i.e., to the belly of the plane. The centre of pressure was, therefore, assumed to be initially at the point on the belly of the plane where the nose strut was located. Note that R is a function of θ, since as the plane rotates, the fulcrum for the rotation (and hence the centre of pressure) moves from the nose strut toward the nose cone. To take this into account, the contour of the front of the plane, from the cowl to the nose cone, was modelled as a parabola. Points on the contour were digitised from a high definition digital side view image of a plane of the model and linear regression was performed to obtain the parabolic coefficients. The parabolic model accounted for 98% of the variance, indicating, that it represented the contour almost perfectly. Plane dimensions and centre of gravity location were obtained from the company aircraft manual which were used to determine the initial value (before the plane began to rotate) of R (1.35 m) and the initial value of θ (31.5°). Witness accounts reported the plane's speed to be between 60 and 65 knots (30.9–33.4 m/s) at the time of landing.

The minimum deceleration needed to create a net clockwise torque and initiate clockwise rotation of the plane can be determined by setting equation (1) equal to zero and substituting the initial value of θ. This gives a value of –16.0 m/s^2, i.e., the deceleration must exceed –16.0 m/s^2 to initiate clockwise rotation. Therefore, the deceleration was assumed to be at least –16.1 m/s^2. A deceleration of –16.1 m/s^2, together with a stopping distance of 30 m predicts an initial velocity of the centre of gravity of 31.1 m/s at the beginning of the furrow, based on the following equation of uniform motion.

$$v = \sqrt{2as} \tag{2}$$

This agrees well with the estimated landing speed from witness accounts. Therefore, it was assumed that the plane decelerated uniformly at –16.1 m/s^2 and that its velocity at the onset of deceleration was 31.1 m/s. The moment of inertia of the plane about its centre of gravity was estimated based on the following equation adapted from Roskam (1985).

$$I = \frac{mL^2 r^2}{4} \tag{3}$$

where m is the mass of the plane, L is its length and r is the radius of gyration for an axis passing through the centre of gravity and parallel to the wing. The company aircraft manual gives the plane's length as 8.61 m. The radius of gyration for a similar aircraft was published in Table B2 of Roskam (1985) and was accordingly assumed to be 0.356. Note that it is not necessary to know the mass of the plane when solving equation (1) since the mass term appears on both sides of the equation. It is necessary to determine the time interval for deceleration in equation (1) since $a = 0$ after that time. The time can be calculated by solving for t in the following equation for uniform motion.

$$s = vt + 0.5at^2 \tag{4}$$

Given that the distance s is 30 m, the initial velocity v is 31.1 m/s and the acceleration a is –16.1 m/s^2, t is equal to 1.86 s. Equation (1) can be solved as a function of time for phases C and D. In Phase C, the plane decelerates and begins to rotate about its centre of pressure (Figure 4). After the plane stops its horizontal sliding in Phase D, it continues to rotate due to its angular momentum, although its angular velocity decreases until the plane is vertical, due to the counter clockwise torque created by the vertical ground reaction force. However, once it passes the vertical orientation, the torque created by the vertical ground reaction force reverses direction and the plane continues to rotate clockwise with increasing angular velocity until the leading edge of the wing impacts the ground, 2.5 s following the onset of horizontal sliding.

The forces experienced by the passenger during Phase C can be separated into a radial force pushing the passenger against the seat back and a tangential force pushing the passenger against the seat cushion. The radial force is produced by the component of the horizontal deceleration normal to seat back and the angular velocity of the plane. The passenger's mass was 86.5 kg from which his upper body mass was estimated to be 58.7 kg, based on body proportions taken from Winter (2009). Using this value for upper body mass, the maximum radial force was 1296 N and minimum was 807 N, sufficient to prevent flexion of the trunk, i.e., sufficient to keep the trunk pushed back against the seat.

The tangential force created a posterior axial load (Figure 3(a)) on the passenger's spine. The maximum posterior axial load was 2459 N and the minimum was 499 N. Although the maximum posterior axial load slightly exceeds the mean failure load for 50% probability of anterior wedge fracture in Table 1, the overall load during Phase C is an axial load combined with an extension moment produced by the radial force, whereas the data in Table 1 were taken from studies in which the axial load was combined with a flexion moment. Furthermore, since the posterior axial load was less than the mean failure load plus one standard deviation, it is unlikely that an anterior wedge compression fracture would have occurred during Phase C.

4.4 Phase D: plane flip and impact

In Phase D, the plane lands flat on its wing, as described in Section 2.1. During this phase, the passenger came to hit the ceiling of the aircraft. Based on the information that the passenger's seatbelt failed during the crash, it is possible to suggest two possible scenarios, which provide a range for the impact force.

In the first situation, referred to as Scenario D1, the seatbelt fails a short time following the end of the plane's rotation and impact with the ground. The passenger is released from his seat while upside down, drops and impacts the ceiling of the aircraft. In this scenario, his fall can be modelled as starting from rest and accelerating due to gravity until making contact with the ceiling.

In the second situation, referred to as Scenario D2, the seatbelt is assumed to fail prior to or at the exact instant of the aircraft's wing hitting the ground. The passenger begins to drop from his seat to the ceiling of the aircraft at the moment the plane makes contact with the ground. Therefore, as opposed to Scenario D1, the passenger hits the ceiling with the combined velocity imparted to him by the plane's rotation and gravitational acceleration.

In both scenarios, the passenger's upper back and/or shoulders impact the plane's ceiling. Upon contact with the ceiling, the passenger's spine would have been subjected to flexion-compression loading. This portion of the incident is illustrated in Figure 7.

Figure 7 Phase D: (a) plane position; (b) passenger position at plane's impact with the ground and (c) impact with the plane's ceiling

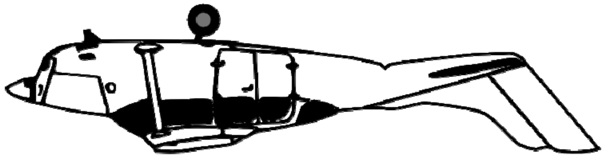

(a)

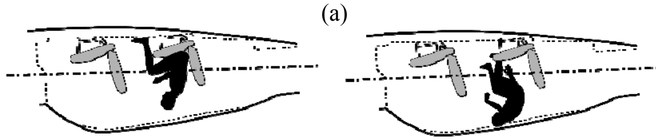

(b)(c)

The fall can be analysed by considering the geometry of the cabin, the size of the passenger and, in the case of Scenario D2, the angular velocity of the plane at impact, which was 3.8 rad/s at the time of impact based on the solution of equation (1). Sudden cessation of the plane's rotation would cause the passenger's torso and head to flex due to the radial deceleration directed towards the front of the plane. It was, therefore, assumed that the passenger fell towards the ceiling of the plane with his neck and torso flexed as shown in Figure 7.

The ceiling of the plane was estimated to be 30 cm from the base of the passenger's neck. In Scenario D1, the vertical velocity of the passenger at the instant of impact with the ceiling would have been 2.43 m/s, based on equation (2) with acceleration set equal to 9.81 m/s^2. The passenger's linear momentum would, therefore, have been 210 kg-m/s. A study conducted with a hybrid cadaveric torso model suggests that the axial compressive force impulse during such an impact has a duration of approximately 40 ms, with the peak occurring less than 10 ms after initial impact (Ivancic, 2013). Approximating the force impulse as having a triangular profile with a duration of 40 ms, gives a peak impact force of 10,500 N.

Figure 8 Stills showing the movements of the buckle necessary to detach the seatbelt strap from its cabin attachment (see online version for colours)

In Scenario D2, the passenger would have had an initial vertical velocity of 13.3 m/s when he began to fall, based on the angular velocity of the plane (3.8 rad/s) and the distance of his seat from the axis of rotation of the plane, estimated to be 3.5 m. At this velocity, it would have taken only 22 ms for his back to hit the ceiling of the aircraft and the velocity at impact would have been 13.5 m/s. The linear momentum would, therefore, have been 1168 kg-m/s. Assuming, the same impact force profile as in Scenario D1, the peak impact force would be 55,900 N. In both, Scenario D1 and D2, it can be assumed that the load would both compress and flex the spine. In both scenarios, the force is well above 99% probability for an anterior wedge fracture based on Table 1, although how much of this force acted in axial compression and how much acted to flex the spine would have depended on the angle of the spine upon impact.

5 Discussion

Based on our analysis, it is not likely that the combination of forces required to cause the L1 anterior wedge fracture occurred during the initial phases (Phase A, B or C) of the emergency landing. However, the combination of forces was likely present at the end of the plane flip (Phase D).

A point to consider is that the passenger of interest was the only occupant to suffer a wedge fracture. While all occupants of the plane were subjected to the same global plane events, only two occupants, including the spine fracture victim, were seated in the second row of seats and were, therefore, exposed to the higher loads generated by the rotation of the plane. When compared to the location of the pilot and co-pilot, these occupants would have been subjected to higher loads based on their distance from the axis of rotation during the flip. However, the second passenger in the back row did not sustain a wedge fracture, nor did their seat belt fail. This further suggests causality between the seatbelt's failure and the subsequent impact with the ceiling during Phase D, both of which were experienced only by the passenger who suffered a wedge fracture.

However, it is also worth noting that the other occupant of the second row did allegedly complain of thoracic level back pain after the incident. This is consistent with our analysis that the anterior wedge fracture did not occur during Phases A, B or C since both passengers would have been subjected to similar forces during those phases. The sudden radial deceleration in Phase D could have been responsible for the soft tissue injury, as this passenger's torso would have been rapidly pitched forward but without impact.

Another important point is that if the passenger who reported the wedge fracture did hit the ceiling of the plane during Phase D, as described, associated injuries such as bruising to the neck, shoulders, back and spinous process areas may have also occurred (Desmoulin and Anderson, 2011). In addition, an upside down fall of this nature would have put the head and neck at risk of injury considering the loads needed to produce fracture are known to be lower in the cervical spine compared to the thoracolumbar junction, although no such injury was reported (Nightingale et al., 2016). From these considerations, Scenario D2 is less likely than Scenario D1. The much higher impact force predicted by Scenario D2 would have been expected to result in more serious injury than an L1 wedge fracture.

The passenger who suffered the wedge fracture was the sole occupant to have his seatbelt fail. Assuming all other safety systems performed as intended with the exception of the seatbelt, the most likely reason for the injury is the seatbelt failure. It should be noted that the seatbelt did not fail due to excessive loading, since it was not damaged, as can be seen in Figure 1. Rather, it failed because it became detached from its anchors. The most probable explanation for the failure would be as the result of accidental detachment by the occupant (or other external factors). In fact, an inspection of the seatbelt in question and the seatbelt attachment point indicated that it is possible to detach the seatbelt with one hand. As shown in Figure 8, a combination of linear and rotational movement can unlatch the carabineer type attachment and release the seatbelt. A failure mechanism this simple should not be tolerated for such a critical safety system and should, therefore, be corrected regardless of whether or not it played a role in the sustained wedge fracture.

6 Conclusion

Using the information available, two scenarios were proposed to account for the injury. Of the two, Scenario D2, in which the seatbelt failed while the aircraft was still rotating, is less likely to have occurred than Scenario D1, where the plane had effectively stopped rotating at the point when the seatbelt failed. Considering that there was no damage to the seatbelt, it is likely that its failure was linked to accidental unlatching of the attachment point. Whether or not this seatbelt failure was the cause of the injury, it is obvious that the impact of the passenger with the ceiling would not have occurred if all of the aircraft's safety systems had performed as intended. Therefore, this suggests a design failure which should be addressed in order that such incidents are not repeated in the future.

Acknowledgements

The authors would like to thank Ms. Christina Stevens (Operations Lead), for her continued support of R&D activities within our company and Mr. Tim Prokop (VP of Development) for turning topics such as this into visually interesting media that support our Science of Violence® course and overall marketing efforts.

References

De Haven, H. (1953) *Development of Crash-Survival Design in Personal, Executive and Agricultural Aircraft*, Cornell-Guggenheim Aviation Safety Center, New York.

Denis, F. (1984) 'Spinal instability as defined by the three-column spine concept in acute spinal trauma', *Clinical Orthopaedics and Related Research*, Vol. 189, pp.65–76.

Desmoulin, G.T. and Anderson, G.S. (2011) 'Method to investigate contusion mechanics in living humans', *Journal of Forensic Biomechanics,* p.2.

Ghobrial, G.M. (2016) *Vertebral Fracture*. [ONLINE] Available at: https://emedicine.medscape.com/article/248236-overview#a7 (Accessed 3 November, 2017).

Greer, D.L., Breeden, J.S. and Heid, T.L. (1964) *Crashworthy Design Principles. General Dynamics*, Convair Div, San Diego, CA.

Hasbrook, A.H. (1969) *Crash Load Vectors in Severe but Survivable Light Plane Accidents (No. 690336)*, SAE Technical Paper.

Huelke, D.F. and Kaufer, H. (1975) 'Vertebral column injuries and seat belts', *The Journal of Trauma*, Vol. 15, No. 4, pp.304–318.

Ivancic, P.C. (2013) 'Hybrid cadaveric/surrogate model of thoracolumbar spine injury due to simulated fall from height', *Accident Analysis and Prevention*, Vol. 59, pp.185–191.

Kim, B.G., Dan, J.M. and Shin, D.E. (2015) 'Treatment of thoracolumbar fracture', *Asian Spine Journal*, Vol. 9, No. 1, pp.133–146.

Myklebust, J., Sances, A., Maiman, D., Pintar, F., Chilbert, M., Rauschning, W., Larson, S., Cusick, J., Ewing, C., Thomas, D. and Saltzberg, B. (1983) *Experimental Spinal Trauma Studies in the Human and Monkey Cadaver (No. 831614)*, SAE Technical Paper.

Nightingale, R.W., McElhaney, J.H., Richardson, W.J. and Myers, B.S. (1996) 'Dynamic responses of the head and cervical spine to axial impact loading', *Journal of Biomechanics*, Vol. 29, No. 3, pp.307–318.

Old, J.L. and Calvert, M. (2004) 'Vertebral compression fractures in the elderly', *American Family Physician*, Vol. 69, No. 1, pp.111–116.

Roskam, J. (1985) *Airplane Design Part V, Component Weight Estimation*. DAR Corporation.

Saber, Y., Jones, J. *et al.* (2017) *Chance Fracture*, [online] Available at: https://radiopaedia.org/articles/chance-fracture (Accessed 9 November, 2017).

Schwinn, D.B. (2014) 'Integration of crashworthiness aspects into preliminary aircraft design', *Applied Mechanics and Materials*, p.598.

Snyder, R.G. (1975) *Crashworthiness Investigation of General Aviation Accidents (No. 750537)*, SAE Technical Paper.

Tuckerman, M. (2019) *Law of Conservation of Energy*, [ONLINE] Available at. http://www.nyu.edu/classes/tuckerman/adv.chem/lectures/lecture_2/node4.html (Accessed 9 November, 2017).

Winter, D., 2009', *Biomechanics, Motor Control of Human Movement*, 4th ed., John Wiley & Sons, Hoboken, New Jersey, USA.

Yoganandan, N., Nahum, A.M. and Melvin, J.W. (Eds.) (2014) *Accidental Injury: Biomechanics and Prevention*, Springer, New York, USA.

Yoganandan, N., Pintar, F., Sances, A., Maiman, D., Myklebust, J., Harris, G. and Ray, G. (1988) *Biomechanical Investigations of the Human Thoracolumbar Spine (No. 881331)*, SAE Technical Paper.